


Impact of novel *N*-aryl piperamide NO donors on NF- κ B translocation in neuroinflammation: rational drug-designing synthesis and biological evaluation

Sajad Shahbazi¹, Jagdeep Kaur¹, Shikha Singh²,
K Gopinath Achary³, Sameena Wani⁴,
Sobhagyalaxmi Jema³, Javed Akhtar³ and
Ranbir Chander Sobti^{1,5}

Innate Immunity
2018, Vol. 24(1) 24–39
© The Author(s) 2017
Reprints and permissions:
sagepub.co.uk/journalsPermissions.nav
DOI: 10.1177/1753425917740727
journals.sagepub.com/home/ini


Abstract

NO donor drugs showed a significant therapeutic effect in the treatment of many diseases, such as arteriopathies, various acute and chronic inflammatory conditions, and several degenerative diseases. NO-releasing anti-inflammatory drugs are the prototypes of a novel class of compounds, combining the pharmacological activities of anti-inflammatory and anti-nociceptive of drugs with those of NO, thus possessing potential therapeutic applications in a great variety of diseases. In this study, we designed and predicted biological activity by targeting cyclooxygenase type 2 (COX-2) and NF- κ B subunits and pharmacological profiling along with toxicity predictions of various *N*-aryl piperamides linked via an ester bond to a spacer that is bound to a NO-releasing moiety (-ONO₂). The result of absorption, distribution, metabolism and excretion and Docking studies indicated that among 51 designed molecules PA-3'K showed the best binding potential in both the substrate and inhibitory binding pocket of the COX-2 enzyme with affinity values of -9.33 and -5.12 for PDB ID 1CVU and 3LNI, respectively, thereby having the potential to be developed as a therapeutic agent. The results of cell viabilities indicated that PA-3'k possesses the best cell viability property with respect to its dose (17.33 ng/ml), with 67.76% and 67.93% viable cells for CHME3 and SVG cell lines, respectively.

Keywords

Nitric oxide, Alzheimer's disease, *N*-aryl piperamides, cyclooxygenase type 2, ADMET, docking

Date received: 25 May 2017; revised: 17 September 2017; accepted: 12 October 2017

Introduction

Non-steroidal anti-inflammatory drugs (NSAIDs) combine the pharmacological activities of anti-inflammatory and antinociceptive effective drugs with NO's biological effects, such as vasodilation, antiaggregation, antimicrobial and immune modulation, resulting in potential therapeutic applications in a wide variety of diseases.¹ In general, most NO donor drugs have been obtained by linking a NO-releasing moiety to druggable molecules by means of a spacer molecule.² The modification of druggable molecules containing NO can provide potent drugs that mainly lack

¹Department of Biotechnology, Panjab University, Chandigarh, India

²Center of Biotechnology, Siksha O Anusandhan University, Khandagiri, Bhubaneswar, Odisha, India

³Imgenex India, E5, Infocity, Bhubaneswar, Odisha, India

⁴Department of Experimental Medicine and Biotechnology, Postgraduate Institute of Medical Education and Research, Chandigarh, India

⁵Babasaheb Bhimrao Ambedkar University, Lucknow, India

Corresponding author:

Sajad Shahbazi, Department of Biotechnology, Panjab University, Chandigarh, 160014, India.
Email: sajad642008@gmail.com



gastrointestinal toxicity and fewer side effects. The cytoprotection of NO release in the gastrointestinal mucosa is due to antagonization of the effect of cyclooxygenase (COX) inhibition through the induction of mucosal vasodilation, inhibition of leukocyte adhesion and margination, and inhibition of mucosal cell apoptosis mediated by caspase inactivation, leading to the slow release of free COX inhibitors in the gastrointestinal mucosa.³

A large number of *in vitro* and *in vivo* pharmacological studies have confirmed the particular anti-inflammatory potential of hybrid drugs.⁴ They recommended the use of NO donor drugs (NODs) for treating different disorders, such as various forms of arthritis colitis and irritable bowel disease; neuroinflammatory diseases (above all, Alzheimer's disease); different pain syndromes; atherosclerosis and thrombotic disorders; calcium and bone metabolism diseases; arterial hypertension; and cancer.^{5,6} In neuroinflammation and cerebral ischemia, particularly reperfusion, NF- κ B translocation into the core and ischemic penumbra, as well as into the microvessels of the affected region.^{6,7} NF- κ B is a key regulator of innate immunity, inflammation and of cell survival and proliferation.⁸ This inducible transcription factor is comprised of two subunits. There are five subunits that can be combined to yield homo- or heterodimers of NF- κ B, as follows: p50, p52, c-Rel, p65 (RelA) and RelB.⁹ Over-activation of NF- κ B after ischemia has been documented in neurons, astrocytes, microglia and in endothelial cells.^{10,11} In neurons, NF- κ B translocation has been associated with apoptosis, whereas in glia and in vascular endothelium, NF- κ B activates a pro-inflammatory phenotype.^{12,13} Therefore, blocking inflammatory phenotype activation of NF- κ B could disrupt the cascade of events that culminates in the pro-inflammatory brain tissue destruction.

In human endothelial cells, the addition of exogenous NO through NODs limits TNF- α activation of NF- κ B in a time- and concentration-dependent manner.¹⁴ In astrocyte and microglia, NODs also exhibit an anti-inflammatory profile through down-regulation of NF- κ B and mitigate iNOS production by inhibiting the ability of NF- κ B to bind to DNA.¹⁵ Inhibition of DNA-NF- κ B may be as a result of direct interaction of NOD with Lys221 and Lys218 of the RelA subunit and protecting them from acetylation.¹⁶ By inhibiting activation of the transcription factor, NO effectively blocks monocyte adhesion, as well as the expression of the pro-inflammatory target genes of NF- κ B, such as TNF- α , IL-6, iNOS, V-CAM, ICAM-1, E-selectin and COX-2.¹⁷ Also, exogenous NO increases mRNA I κ B levels and stabilizes the complex formed with NF- κ B.¹⁵ This stabilization is related to S-nitrosylation of the Cys179 of IKK- β , which decreases its ability to phosphorylate I κ B.¹⁸ Additionally, NO interferes with the transient

degradation of I κ B- α induced by cytokines.¹⁹ These three actions induce negative regulation of NF- κ B DNA-binding activity by NOD.²⁰

In neuroinflammation and degeneration, activation of NF- κ B occurs, at least in part, via ROS.²⁰ Earlier, it was shown that one of the most significant sources of ROS in the ischemic brain is obtained through the metabolism of arachidonic acid by COX.²¹ The COX-2 expression is increased in brain tissue after global and focal cerebral ischemia.²² ROS are produced in the prostaglandin G2 to H2 conversion process by the peroxidase step of the COX reaction.²³ Therefore, the reduction in COX-2 activity can alleviate the oxidative damage of the ischemic brain.²⁴ The NO donors, which are able to down-regulate LPS-induced COX-2 protein activity or protein expression through binding to the active site of a protein, or via inhibition of NF- κ B DNA binding activity in murine monocytes, may be candidates for neuroprotective antioxidants in cerebral ischemia.²⁵ The mode of action of COX-2 inhibitor NODs is depicted in Figure 1. Inhibition of NF- κ B can be direct or indirect. The former can be obtained by binding drugs to NF- κ B's subunits and directly suppressing the NF- κ B assembling and activity.²⁶ The latter can take place by inhibiting the interaction of the p65 subunit to the shuttles, such as AKIP 1A, responsible for translocation of the NF- κ B-shuttle complex into nucleus.²⁷ Indirect NF- κ B inhibition occurs through activated or deactivated receptors in its pathways like the effect of NO to down-regulate and suppress NF- κ B activity.²⁷

As a series of detailed reviews of the new NO donors, in general, and NO hybrid drugs pharmacological properties, in particular, have already been published,²⁸ it could be useful here to focus on recent drug developments with natural-based molecules (NBMs). Among all NBMs, piperine-based molecules have been selected. Piperine is an alkaloid extracted from black pepper (scientific name), which has a wide range of applications in industry and pharmacy.²⁹ There are many reports about various derivatives of piperine and its pharmacological and physiochemical properties.³⁰ Among all derivatives, *N*-aryl piperamides have shown significant anti-inflammatory activity in both *in vitro* and *in vivo* studies.³¹ Owing to the reportedly excellent anti-inflammatory activities of such compounds, in this study, we selected *N*-aryl piperamides as the basic structures with which to develop novel NO donors for treatment of neuroinflammatory diseases. The ability of exogenous NO to inhibit the nuclear shift of NF- κ B and down-regulate the expression of pro-inflammatory and inflammatory cytokines in the inflammation pathway, combined with the brilliant capabilities of *N*-aryl piperamides to inhibit COX enzymes, can provide promising candidates for anti-neuroinflammatory NOD development.

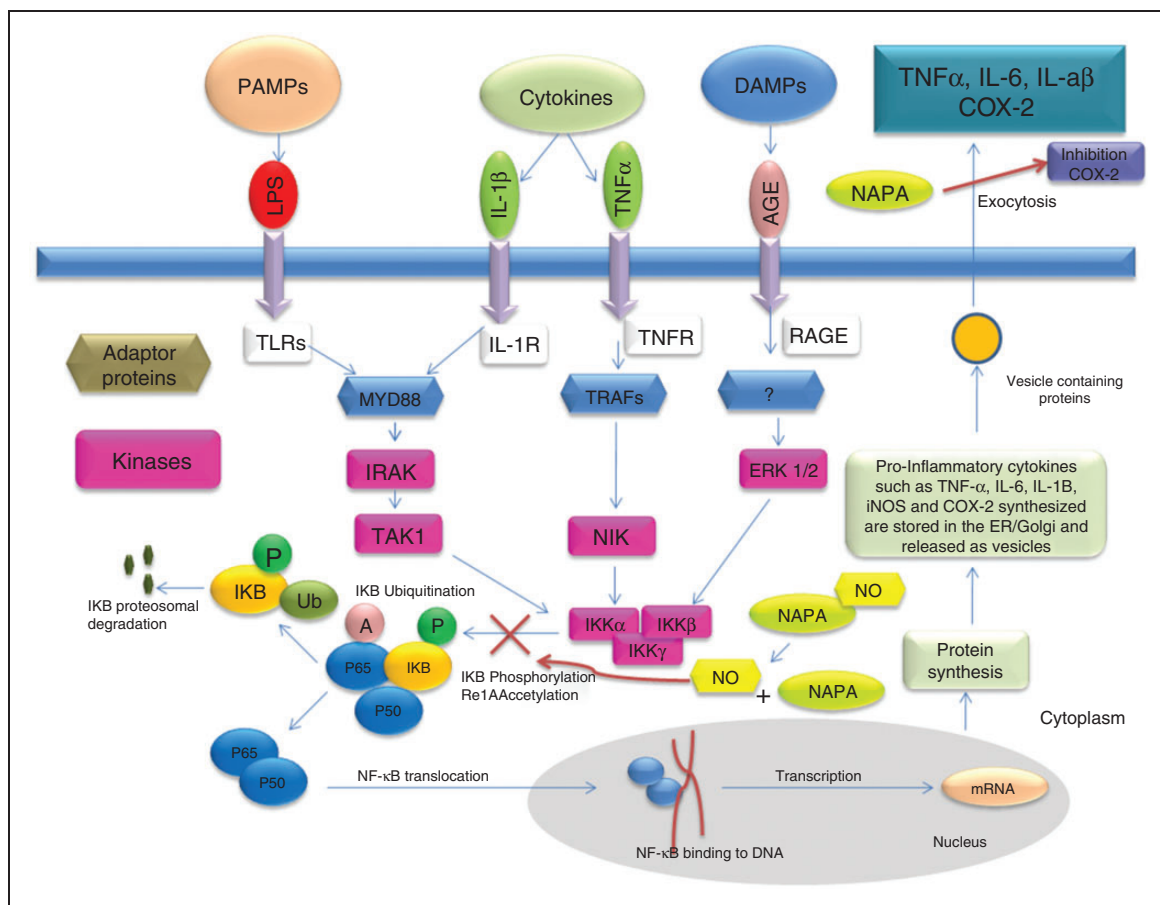


Figure 1. Schematic diagram of the NF- κ B pathway and the inhibitory effect of various alkyl nitrate N-Aryl Piperamide on NF- κ B translocation and COX-2 function. Membrane receptors including TLRs, tumor TNFR, IL-1R and RAGE recognize stimuli like PAMPs, DAMPs and cytokines which activate proteins such as TNF associated factors (TRAF) and myeloid differentiation primary response protein 88 (MyD88). TRAF and MyD88 activate protein kinases such as MAPK such as ERK1/2, NIK, TAK1, and IRAK. These kinases cause phosphorylation of I κ B- α via activating I κ B kinases (IKK α , IKK β and IKK γ). This process causes the breakage the I κ B- NF- κ B complex and nuclear translocation of NF- κ B to binds to specific DNA. Nuclear translocation motivate the expression of pro-inflammatory cytokines, inflammatory cytokines, adhesion molecules, Cyclooxygenase-2 and iNOS. Alkyl nitrate N-aryle piperamides (NAPA-ONO₂) release and increase the amount of NO in site of inflammation. High amount of NO results in acetylation protection of Lys221 & Lys218 of RelA, Stabilization of NF-KB via decreasing phosphorylation of I κ B by S-nitrosylation of Cys179 of IKKB and Interfere transient degradation of I κ B- α , in turn, inhibiting the I κ B- NF- κ B complex breakage, ceasing the NF- κ B translocation and reducing or completely stopping the pro-inflammatory and inflammatory cytokines expression. Additionally NAPA itself is capable to interact with COX-2 enzyme and inhibit it directly. Figure has been modified from Fihuera-Losada et al., 2014 (doi: 10.3389/fnmol.2015.00024).

Materials and methods

In silico drug designing

Designing of various N-aryl-alkyl nitrate amide derivatives of piperine. All chemical structures were drawn and designed with ChemBioDraw 12.0 (Cambridgesoft chemoffice suite 2009) and saved in MDL Molfile format. Various derivatives of piperine have been designed by interacting of primary amine moiety (different anilines) with three types of primary alkyl halide nitrate (1-bromomethyl nitrate, 2-bromoethyl nitrate, 3-bromopropyl nitrate) in the first step. Then different amides interacted with piperic acid to form various alkyl nitrate derivatives of N-aryl piperamides.

Druggability and absorption, distribution, metabolism and excretion studies. The study of absorption, distribution, metabolism and excretion (ADMET) was performed via the Qikprop 3.4 module of Schrodinger Suite 2011 (Qik Prop, 2011, Version 3.4; Schrödinger, New York, NY, USA). The pharmacokinetic profiles of the compounds were assessed by the #start parameter, which indicates the number of property descriptors out of range for 95% of known drugs.³² These criteria included SASA, FOSA, FISA, volume, PISA, Glob, Metab, QPlogKhsa, mol_MW, donorHB, acctpHB, QPlogPo/w, QPlogPw, QPlogPoct, and QPlogPC16,³³ CNS, the human oral absorption level, the maximum transdermal transport rate (Jm), QPlogHERG,

QPlogBB, QPPCaco, QPPMDCK, QPlogKp, IP(eV), EA(eV) and the number of violations of Lipinski's rule of five of the different alkyl nitrate derivatives of various *N*-aryl piperamides.³⁴

The toxicity of compounds was estimated via the online TOPKAT approaches of Accelrys Environmental Chemistry and Toxicology Workbench (Accelrys, San Diego, CA, USA; <https://ect01.accelrys-online.com/webport/ECT/main.htm>). TOPKAT has predicted the toxicity profiling of compounds, including Mutagenicity (Ames test v3.1), Rodent Carcinogenicity from the FDA dataset for both female and male (v3.1), Skin Sensitization (GPMT) (v.6.1), Skin Irritancy (v6.1), Ocular Irritation (v5.1), Weight Of Evidence (WOE) (v5.1), Developmental Toxicity Potential (DTP) (v5.1), Aerobic Biodegradability (v6.1), EC50 (half of effective concentration), LD50 (half of lethal dose), LC50 (half of lethal concentration) and TD50 (half of tolerance dose).³⁴ The ADMET results are listed in Table 1.

Selection and preparation of receptors and druggable ligands. COX-2 structures with PDB IDs of 1CVU and 3LN1, and NF- κ B with PDB IDs of 1NFI, 1SVC, 2RAX, 3EB5 and 3JWE were obtained from the RCSB Protein Data Bank (<http://www.rcsb.org/pdb/>) with X-ray diffraction resolutions of 2.40, 2.40, 2.70, 2.60, 3.30, 2.00 and 2.70 Å, respectively. The retrieved protein preparations were performed via the Protein Preparation Wizard of Schrödinger suite 2011 (Schrödinger Suite; Epik version 2.2; Impact version 5.7; Prime version 2.3).

Druggable compounds were prepared using LigPrep 2.5 module of Schrödinger Suite 2011 using the OPLS force-field 2005 at biologically relevant pH. It was performed by assigning the protonation states, including the disconnection of group I metals in simple salts, the deprotonation of strong acids and the protonation of strong bases, while adding explicit hydrogens and topological duplicates.

Receptor–ligand interactions. Glide 5.7 module in Extra Precision (XP) mode was employed for scoring the docking of ligands and related receptors,^{35,36} and the MMGBSA (the molecular mechanics/generalized born surface area) of each ligand–protein complex was calculated via Prime 3.0 application of Schrödinger Suite 2011.³⁷ The results of docking and MMGBSA are available in Table 2. Then, the complex of receptor–ligand was mapped via XP visualizer approaches of Schrödinger 2011 and the receptor surfaces were configured according to the electrostatic potential of residues in the binding packet of protein by truncating the receptor surface in 5 Å from ligand with 20% transparency. The pose of the ligand was visualized via the Ligand Interaction Diagram module of Schrödinger 2011 and the pose of the selected ligand is represented in Figure 2B.

Selection of potent anti-neuroinflammatory NODs. The ideal compound(s) was (were) selected based on the ADMET profiles within the recommended range for each criterion and highest affinity value(s) for inflammation responsible receptors with PDB IDs 1CVU and 3LN1 and possess(es) better NF- κ B binding affinity. Then the potential candidate(s) will be suggested for further study.

Synthesis (total synthesis methodology)

General procedure of selective primary amine protection (a-q; amine-Boc protection). Three grams of primary amine (various aniline derivatives; a-q) dissolved in water/tetrahydrofuran (THF) 1:1, 3 eq. sodium carbonate (NaHCO_3) were added and the sample was stirred for 30 min at 0°C. Then, 1.2 eq. di-tert-butyl dicarbonate (Boc_2O) was added and the sample was stirred overnight (12 h) at room temperature (RT; 25°C). The organic layer was separated and washed twice with distilled water, then dried over magnesium sulfate (MgSO_4) and purified by flash column chromatography with 2% ethyl acetate/hexane to remove possible impurities. The product comprised whitish crystals with 99–100% yield.

General procedure of amide production (secondary amine; 2 a-q, 3 a-q, 4 a-q). Three grams of Boc-protected primary amine (aniline derivatives; 2 a-q, 3 a-q and 4 a-q) and 10 eq. sodium hydride (NaH) were dissolved in 40 ml dry THF in a double-neck, round-bottom flask, under argon. The sample was stirred for 1 h at 0°C, and 1.5 eq. alkyl dihalide ($\text{Br-C}_n\text{H}_{2n}\text{-Cl}$) was added. After stirring overnight at RT, monitoring via TLC and reaction completion, the sample was neutralized with excess NaH in methanol on ice, then washed with water. The compound was extracted with ethyl acetate, dried over sodium sulfate (Na_2SO_4), evaporated and purified by column chromatography with 5% ethyl acetate/hexane. The product represented an oily liquid with 99–100% yield.

General procedure of amide deprotection and nitration ($\text{O}_2\text{-NO-R}_4$; 2 a-q, 3 a-q, 4 a-q). Boc-protected amides were dissolved in dichloromethane (DCM)/trifluoroacetic acid 1:1, stirred for 5 h at RT and monitored by TLC, then washed and extracted with DCM, dried over MgSO_4 and purified by column chromatography in 5% ethyl acetate/hexane. The product was an oily liquid with 100% yield. The deprotected amide was dissolved in dry acetonitrile (MeCN), and dissolved 2.3 eq. silver nitrate (AgNO_3) in dry MeCN was added portionwise to the amide mixture and stirred for 24–72 h at 70–80°C, except those amides which contained halides in their aryl ring, which were stirred for 72–96 h at 0°C. Samples were monitored by TLC, washed with water and extracted with DCM. The

Table 1. ADME and pharmacodynamic properties.

Title	CNS	MM	Donor HB	Acpt HB	QPlog Po/w	QPlog QPllogS	CIQPlogS	QPlog HERG	QPP Caco	QPlog BB	QPP MDCK	QPlog Khsa	HOA	ROF	ROT	Jm
PA-2'a	-2	450.37	0	7	3.90	-5.21	-6.23	-6.42	305.53	-1.48	599.17	0.03	3	0	0	0.009
PA-2'b	-2	450.37	0	7	3.73	-4.64	-6.23	-6.30	370.52	-1.40	506.02	-0.04	3	0	0	0.063
PA-2'c	-2	400.36	0	7	3.11	-3.94	-5.16	-6.35	340.81	-1.56	237.07	-0.22	3	0	0	0.271
PA-2'd	-2	428.46	0	7.5	3.51	-4.62	-5.53	-6.45	320.11	-1.71	246.21	-0.09	3	0	0	0.047
PA-2'e	-2	426.43	1	8.7	2.78	-4.56	-5.22	-6.44	120.10	-2.37	50.05	-0.08	2	0	0	0.010
PA-2'f	-2	495.37	0	8	3.29	-5.05	-6.72	-6.34	64.88	-2.34	112.45	-0.10	3	1	0	0.001
PA-2'g	-2	426.38	0	8.5	2.31	-2.96	-5.14	-5.95	320.71	-1.63	144.72	-0.56	3	0	0	1.705
PA-2'h	-2	442.42	0	8.5	3.09	-4.08	-5.36	-6.36	319.79	-1.89	144.27	-0.29	3	0	0	0.165
PA-2'i	-2	440.41	0	8.5	2.73	-3.71	-5.43	-6.19	320.05	-1.70	144.40	-0.37	3	0	0	0.294
PA-2'j	-2	412.40	0	7.75	2.95	-3.81	-5.07	-6.34	320.00	-1.77	144.37	-0.29	3	0	0	0.319
PA-2'k	-2	412.40	1	8.7	2.39	-4.09	-4.94	-6.39	98.70	-2.43	40.49	-0.22	2	0	0	0.020
PA-2'l	-2	382.37	0	7	2.88	-3.40	-4.78	-6.23	419.60	-1.50	193.50	-0.30	3	0	0	1.522
PA-2'm	-2	416.82	0	7	3.41	-4.37	-5.51	-6.29	358.20	-1.46	402.53	-0.15	3	0	0	0.093
PA-2'n	-2	461.27	0	7	3.48	-4.13	-6.46	-6.08	494.20	-1.25	613.06	-0.17	3	0	0	0.335
PA-2'o	-2	427.37	0	8	2.14	-3.28	-5.27	-6.06	59.08	-2.50	23.25	-0.42	2	1	0	0.040
PA-2'p	-2	412.40	0	7.75	2.96	-3.38	-5.07	-6.04	494.55	-1.50	231.11	-0.35	3	0	0	1.954
PA-2'q	-2	427.37	0	8	2.34	-3.11	-5.27	-6.13	119.70	-2.14	49.88	-0.45	3	1	0	0.305
PA-3'a	-2	464.40	0	7	4.31	-5.68	-6.52	-6.61	305.09	-1.59	598.38	0.16	3	0	0	0.004
PA-3'b	-2	464.40	0	7	4.09	-4.94	-6.52	-6.43	406.58	-1.45	522.77	0.07	3	0	0	0.051
PA-3'c	-2	414.39	0	7	3.48	-4.43	-5.46	-6.60	318.53	-1.72	208.50	-0.08	3	0	0	0.106
PA-3'd	-2	442.49	0	7.5	3.89	-5.05	-5.83	-6.59	317.04	-1.82	243.65	0.04	3	0	0	0.022
PA-3'e	-2	440.45	1	8.7	3.15	-4.95	-5.50	-6.59	118.88	-2.49	49.51	0.03	2	0	0	0.005
PA-3'f	-2	509.40	0	8	3.69	-5.48	-7.01	-6.48	64.68	-2.47	112.06	0.03	2	2	0	0.000
PA-3'g	-2	440.41	0	8.5	2.70	-3.39	-5.43	-6.11	317.71	-1.73	143.25	-0.43	3	0	0	0.793
PA-3'h	-2	456.45	0	8.5	3.48	-4.53	-5.66	-6.51	316.88	-2.00	142.85	-0.15	3	0	0	0.075
PA-3'i	-2	454.44	0	8.5	3.14	-4.24	-5.73	-6.43	304.87	-1.84	137.01	-0.23	3	0	0	0.104
PA-3'j	-2	426.43	0	7.75	3.34	-4.25	-5.37	-6.49	316.99	-1.88	142.90	-0.16	3	0	0	0.147
PA-3'k	-2	426.43	1	8.7	2.78	-4.57	-5.22	-6.62	94.12	-2.59	38.46	-0.10	2	0	0	0.008
PA-3'l	-2	396.40	0	7	3.28	-4.11	-5.08	-6.61	317.03	-1.78	142.92	-0.13	3	0	0	0.236
PA-3'm	-2	430.84	0	7	3.79	-4.88	-5.81	-6.52	317.23	-1.64	353.10	0.00	3	0	0	0.030
PA-3'n	-2	475.30	0	7	3.87	-5.01	-6.75	-6.55	317.19	-1.63	379.61	0.03	3	0	0	0.024
PA-3'o	-2	441.40	0	8	2.53	-4.15	-5.57	-6.52	37.94	-2.96	14.40	-0.23	2	1	0	0.003
PA-3'p	-2	426.43	0	7.75	3.34	-4.26	-5.37	-6.50	317.02	-1.88	142.92	-0.16	3	0	0	0.144
PA-3'q	-2	441.40	0	8	2.68	-3.91	-5.57	-6.48	69.04	-2.60	27.51	-0.26	2	1	0	0.020
PA-4'a	-2	478.42	0	7	4.70	-6.14	-6.82	-6.78	305.14	-1.70	598.48	0.30	3	0	1	0.002
PA-4'b	-2	478.42	0	7	4.52	-5.57	-6.82	-6.67	367.04	-1.61	500.86	0.23	3	0	0	0.012
PA-4'c	-2	428.42	0	7	3.90	-4.86	-5.76	-6.71	337.52	-1.78	234.59	0.05	3	0	0	0.053
PA-4'd	-2	456.51	0	7.5	4.32	-5.63	-6.12	-6.84	304.93	-1.96	233.58	0.19	3	0	0	0.007
PA-4'e	-2	454.48	1	8.7	3.74	-6.00	-5.79	-7.18	118.77	-2.75	49.45	0.22	3	0	1	0.001
PA-4'f	-2	523.42	0	8	4.11	-5.83	-7.31	-6.61	79.41	-2.46	140.32	0.15	2	2	1	0.000
PA-4'g	-2	454.44	0	8.5	3.10	-3.88	-5.73	-6.32	317.17	-1.85	142.99	-0.29	3	0	0	0.329
PA-4'h	-2	470.48	0	8.5	3.82	-4.73	-5.96	-6.45	316.53	-2.05	142.68	-0.04	3	0	0	0.056
PA-4'i	-2	468.46	0	8.5	3.52	-4.64	-6.02	-6.54	316.62	-1.92	142.72	-0.10	3	0	0	0.056
PA-4'j	-2	440.45	0	7.75	3.74	-4.73	-5.67	-6.68	316.57	-1.99	142.70	-0.02	3	0	0	0.062
PA-4'k	-2	440.45	1	8.7	3.15	-4.99	-5.50	-6.79	93.47	-2.72	38.18	0.01	2	0	0	0.004
PA-4'l	-2	410.43	0	7	3.54	-4.24	-5.38	-6.43	308.12	-1.84	138.58	-0.04	3	0	0	0.169
PA-4'm	-2	444.87	0	7	4.05	-5.01	-6.11	-6.34	307.84	-1.70	341.78	0.09	3	0	0	0.021

(Continued)

Table 1. Continued.

Title	CNS	MM	Donor HB	Acpt HB	QPlog Po/w	QPlogS	CIQPlogS	QPlog HERG	QPP Caco	QPlog BB	QPP MDCK	QPlog Khsa	HOA	ROF	ROT	Jm
PA-4'n	-2	489.32	0	7	4.19	-5.15	-7.05	-6.40	338.79	-1.65	406.89	0.13	3	0	0	0.022
PA-4'o	-2	455.42	0	8	2.83	-4.38	-5.87	-6.39	37.04	-3.03	14.04	-0.12	2	1	0	0.002
PA-4'p	-2	440.45	0	7.75	3.74	-4.63	-5.67	-6.62	351.12	-1.92	159.60	-0.04	3	0	0	0.096
PA-4'q	-2	455.42	0	8	3.10	-4.16	-5.87	-6.55	96.33	-2.52	39.44	-0.16	2	1	0	0.028

CNS, central nervous system activity -2, -1, 0, 1, 2: -2, completely inactive, -1, very low activity, 0, low activity, 1, medium activity, 2, completely active; MM, molecular mass: recommended value (R.V.): 130-725; DonorHB, estimated number of hydrogen bonds that would be donated by the solute to water molecules in an aqueous solution: R.V. = 0.0-6.0; AcptHB, estimated number of hydrogen bonds that would be accepted by the solute from water molecules in an aqueous solution: R.V. = 2.0-20.0; QPlogS, prediction aqueous solubility level, recommended range $-6.5 < x < 0.5$; CIQPlogS, conformation-independent predicted aqueous solubility, $-6.5 < x < 0.5$; QPlogPo/w, predicted octanol/water partition coefficient: R.V. = -2.0 to 6.5; QPlogHERG, predicted IC50 value for blockage of HERG K+ channels; < -5 = concern; QPPCaco, predicted apparent gut-blood barrier permeability, < 25 = poor, > 500 = high; QPlogBB, predicted brain/blood partition coefficient, -3.0 to -1.2; QPPMDCK, predicted apparent MDCK cell permeability, < 25 = poor, > 500 = high; QPlogKhsa, prediction of binding to HSA; -1.5 to 1.5; Metab, number of likely metabolic reactions, 1-8; HOA, human oral absorption level, 1, 2, 3: 1 = low, 2 = medium, 3 = high; ROF, the number of violations of Lipinski's RO5; SL, solubility level, 0, 1, 2, 3, 4, 5: 0 = extremely low, 1 = very low, 2 = low, 3 = good, 4 = optimal, 5 = too soluble; ROT, the number of violations of Jorgensen's RO3; Jm, maximum transdermal transport rate.

Table 2. Docking score and MMGBSA energy of ligands-receptors complexes.

Title	COX-2				NF-kB											
	ICVU		3LNI		INFI		ISVC		2RAX		3EB5		3JWE			
	XP	DG	XP	DG	XP	DG	XP	DG	XP	DG	XP	DG	XP	DG		
PA-2'd	-5.93	-55.94	-0.64	-46.84	-2.03	-49.18	-1.33	-48.29	-2.95	-35.53	-1.08	-53.46	-0.38	-47.08		
PA-2'e	-6.01	-54.40	-3.11	-51.90	-2.46	-41.02	-1.95	-40.88	-3.31	-27.90	-0.69	-60.99	-1.36	-41.47		
PA-2'f	-5.44	-39.28	-0.95	-12.99	-0.55	-40.76	-1.87	-33.24	-1.78	-27.11	1.08	-24.03	0.44	-35.52		
PA-2'i	-5.60	-30.03	-1.68	-38.55	-1.99	-44.47	-1.66	-35.43	-2.67	-38.91	0.49	-26.94	-1.15	-33.50		
PA-2'k	-5.36	-56.32	-2.07	-47.21	-2.67	-41.52	-2.61	-39.42	-1.76	-40.62	-1.72	-59.87	-1.46	-41.87		
PA-2'o	-5.59	-56.21	-1.35	-29.69	-1.82	-40.71	-2.10	-39.18	-3.03	-35.43	2.09	-50.42	-0.77	-37.77		
PA-2'p	-6.49	-49.63	-2.11	-38.35	-1.75	-40.24	-0.84	-30.50	-2.93	-42.07	-1.22	-43.31	-0.77	-44.69		
PA-2'q	-5.48	-53.68	-2.12	-40.11	-1.03	-44.41	-2.55	-39.39	-1.28	-26.12	-1.54	-45.31	-0.62	-44.38		
PA-3'd	-5.86	-47.09	1.93	-33.88	-1.79	-48.80	-2.71	-51.02	-2.51	-41.54	0.32	-68.66	-1.10	-47.03		
PA-3'e	-6.06	-48.45	-3.67	-43.16	-2.20	-41.24	-1.79	-42.52	-4.02	-46.31	-1.21	-64.74	-2.05	-50.55		
PA-3'i	-6.57	-44.64	-0.16	-48.31	-1.18	-46.19	-2.07	-37.38	-0.70	-27.57	-0.40	-59.85	-0.40	-39.93		
PA-3'k	-5.95	-53.98	-4.25	-51.31	-1.99	-39.64	-1.40	-39.47	-3.61	-51.18	-0.51	-58.61	-2.29	-41.29		
PA-3'o	-5.97	-56.12	-1.28	-39.89	-1.49	-45.88	-1.09	-49.41	-2.62	-31.41	0.56	-62.35	-0.87	-38.09		
PA-3'p	-4.18	-53.61	-1.99	-23.52	-2.97	-40.62	-2.43	-43.91	-2.16	-38.09	2.06	-48.51	-0.20	-54.38		
PA-3'q	-5.01	-58.42	-1.21	-28.08	-1.05	-44.13	-2.24	-42.36	-1.82	-32.41	-0.17	-50.68	-0.85	-40.39		
PA-4'c	-4.67	-46.95	-2.32	-34.99	0.93	-35.97	-0.16	-31.75	-2.65	-43.07	-1.33	-53.47	-0.85	-41.15		
PA-4'd	0.00	0.00	-2.96	-49.82	-0.79	-52.75	-1.28	-41.58	-3.03	-47.33	1.46	-57.59	-2.18	-55.99		
PA-4'g	-6.13	-48.83	-2.66	-46.74	-1.72	-45.55	-1.47	-33.88	-2.36	-43.00	-0.17	-50.77	-0.69	-42.73		
PA-4'h	-5.54	-51.28	-2.49	-40.94	-2.99	-44.73	-2.01	-40.92	-2.14	-44.41	-0.68	-45.04	-1.51	-48.44		
PA-4'i	-5.37	-57.62	-1.08	-39.74	-1.64	-42.41	-2.03	-42.35	-2.56	-39.49	-0.75	-56.71	-1.27	-48.01		
PA-4'j	-5.94	-50.86	-2.29	-54.32	-3.11	-41.35	-2.92	-46.66	-2.80	-51.34	0.63	-50.77	-1.31	-40.10		
PA-4'k	-5.90	-45.13	-4.18	-51.53	-2.34	-49.58	-3.10	-36.55	-3.07	-49.61	0.21	-61.74	-1.49	-41.75		
PA-4'l	-5.64	-54.93	-3.84	-49.38	-0.48	-45.25	-0.64	-34.03	-2.55	-43.72	1.36	-58.09	-0.89	-33.07		
PA-4'o	-6.07	-46.48	-1.03	-32.58	-2.36	-41.80	-0.62	-46.44	-2.61	-47.35	0.10	-60.95	-1.43	-44.61		
PA-4'p	-5.38	-51.20	-1.32	-31.03	-1.96	-23.82	-2.12	-50.75	-0.12	-24.49	-0.81	-60.97	-2.06	-50.15		
PA-4'q	-4.44	-46.19	-1.72	-32.17	2.59	-40.90	-2.00	-34.83	-2.51	-39.94	-2.35	-53.41	-0.61	-37.26		
Aspirin	-5.19	-21.12	-4.43	-23.66	-4.60	-27.63	-2.27	-11.17	-1.52	-8.64	-3.94	-27.14	-3.49	-27.90		

(Continued)

Table 2. Continued.

Title	COX-2				NF-kB											
	1CVU		3LN1		INFI		ISVC		2RAX		3EB5		3JWE			
	XP	DG	XP	DG	XP	DG	XP	DG	XP	DG	XP	DG	XP	DG		
Celecoxib	—		-11.71	-89.33	-1.61	-36.45	-2.93	-38.23	-3.85	-43.15	-2.49	-45.67	-2.08	-40.06		

DG (ΔG_{bind}) = Gcomplex - (Gprotein + Gligand) where ΔG_{bind} is ligand binding energy; XP Gscore: Extra Precision Glide score.

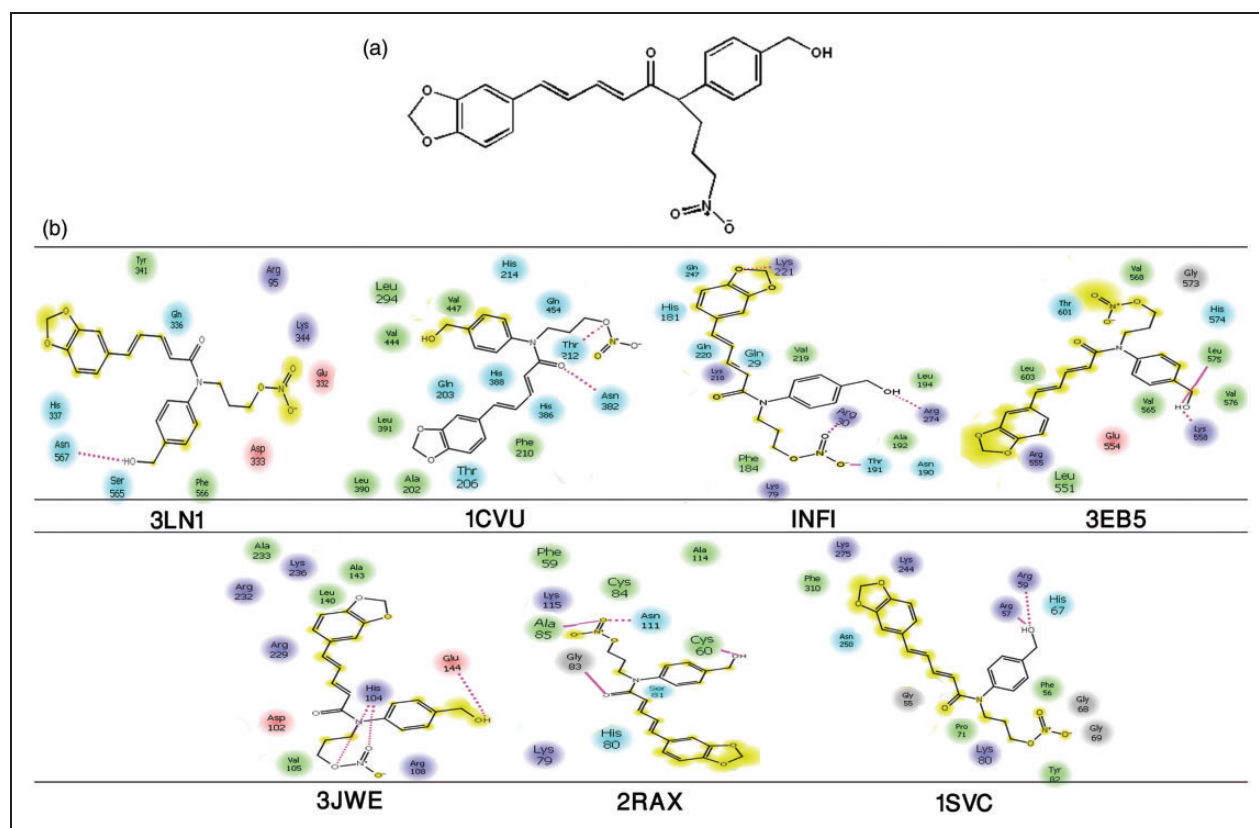


Figure 2. (A) The 2D structures of PA-3'k (B) The 2D structures of PA-3'k in binding pockets of receptors [PDB IDs: 3LN1, 1CVU, p65 (INFI), 3EB5, 3JWE, 2RAX and 1SVC]. The pose of the ligand in binding pockets and chemical characterization of residues are depicted where cyan, green and purple indicate polar, hydrophobic and positively charged amino acids, respectively. All hydrogen bonds are shown by the pink dashed line.

extracts were washed two more times with water and the organic layers were dried over NaSO_4 and purified by flash column chromatography. The resulting product represented a dark oily liquid in a yield of 90–100%.

Hydrolyzation of piperin to piperic acid (1). Fifteen grams of piperin were dissolved in 20% methanolic potassium hydroxide (KOH), refluxed for 72 h at 80°C , then evaporated, which yielded a yellowish potassium piperate. To this sample, 500 ml hot water was added and acidified by adding dropwise con. HCl, then shaken and left for 30 min at RT, washed with water and filtered by

applying a vacuum, and re-crystallized with ice-cold methanol or dry THF. The product was a yellow crystal with mp. 218°C , and 88% yield.

General procedure for production of alkyl nitrate derivatives of N-aryl piperamide (PA-2'a-q, PA-3'a-q, PA-4'a-q). Three grams of piperic acid was dissolved in dry DCM, 1 eq. of freshly distilled thionyl chloride (SOCl_2) was added at 0°C and the sample was stirred for 3–4 h at RT (1'). Then, 1 eq. of aryl-amide-alkyl-nitrate was added, as well as 2.3 eq. of Hünig's base (*N,N*-di-isopropylethylamine) at 0°C . The sample was stirred for

24–72 h at RT and purified by column chromatography in 20% methanol/DCM. The yield was 78–90%.

All physicochemical properties, characteristics and *in vitro* biological data will be published in a next series of publications. The IUPAC names of compounds are listed in Table S1.

In vitro biological tests

The biological experiments were performed to test a dose-dependent release of the pro-inflammatory cytokines IL-12 and IFN- γ in the extracellular matrix of human microglia (CHME3) and astrocyte (SVG) cell-lines (fourth passage, kindly provided by Dr. A. Basue, National Institute of Brain Research, Manisar, Gurgaon, Inida) via human IL-12 (Abcam, Cambridge, UK) and IFN- γ ELISA kits (Invitrogen, Carlsbad, CA, USA). After 12 and 24 h of LPS treatment, cells were challenged with four selected compounds, i.e. PA-2'p, PA-3'k, PA-4'g and PA-4'o, based on the computed EC₅₀ of each compound. Then, the cell viability and cell inhibitory IC₅₀ for both cell lines were evaluated in selected doses for four druggable candidates via MTT assays (Thiazolyl Blue Tetrazolium Bromide; Sigma Aldrich, St. Louis, MO, USA).

Results and discussion

Designing of various *N*-aryl-alkyl nitrate amide derivatives of piperine

Piperine, the alkaloid responsible for the pungency of black pepper and long pepper, is a yellow crystalline substance, has a melting point of 128–130°C. It is a weak base, which, on hydrolysis with aqueous alkali or nitric acid, yields a volatile base C₅H₁₁N, known as piperidine, and in acidic hydrolysis results in piperic acid (C₁₂H₁₉O₄), with a melting point of 216–218°C was shown to be 5-(3,4-methylenedioxy phenyl)-2,4-pentadienoic acid.

Piperine treatment has also resulted in lower lipid peroxidation *in vivo* and beneficially influenced the cellular thiol status, antioxidant molecules and enzymes in a number of experimental situations of oxidative stress.³⁸ It can be used as an anti-inflammatory, anti-thyroid, growth stimulatory, thermogenic and chemopreventive compound. It also shows antipyretic, analgesic, insecticidal, immunomodulatory, antitumor, anti-depressant and anti-apoptotic activities.³⁹ It strongly inhibits UDP-glucuronyl transferase, and intestinal and hepatic aryl hydrocarbon hydroxylase. Piperine is not only non-genotoxic, but also possesses anti-mutagenic and anti-tumor properties.⁴⁰

Despite all these properties, it is still necessary to modify the piperine structure to improve the pharmacological impact and targeting, by which it can be

considered as an effective and independent drug. Recently, different derivatives of piperine have been designed and synthesized, and their therapeutic capability against a variety of human health complexities has been reported. The aromatic and aliphatic amide derivatives of piperine along with NODs and hybrid drugs showed outstanding effects on different diseases, particularly inflammatory disorders.

Based on such interesting properties of both piperamide and NODs, we designed different aromatic piperamide–NO hybrid compounds. Various alkyl nitrate *N*-aryl piperamides have been designed using ChemBioDraw 12.0. Molecules were prepared by combining the different nitrate alkyl-anilins, resulting from combination of the primary amine moiety (different anilines) with three types of primary alkyl halide nitrate (1-bromomethyl nitrate, 2-bromoethyl nitrate, 3-bromopropyl nitrate) to form various alkyl nitrate *N*-aryl piperamides.

Also, we have developed and standardized the synthesis methodology of such, and the total synthetic scheme is depicted in Figure 3. These compounds have been screened *in silico* for the study of druggability and pharmacological properties.

ADMET prediction

The first step of drug discovery is checking the druggability and pharmacological properties of designed molecules. For the oral administration of druggable compounds, different criteria have to be considered, such as the oral and intestinal absorption level to deliver and distribute via the blood stream, level of metabolism and the ability of excretion from the body, along with toxicogenicity. The Qikprop module of Schrödinger suite introduced the #star parameter, including 24 criteria such as MW, dipole, IP, EA, SASA, FOSA, FISA, PISA, WPSA, PSA, volume, #rotor, donorHB, acptHB, glob, QPpolrz, QPlogPC16, QPlogPoct, QPlogPw, QPlogPo/w, logS, QPLogKhsa, QPlogBB and #metabol. These criteria are commonly used to predict the pharmacokinetic and pharmacodynamic properties of druggable molecules.

The Lipinski's rule of five, known also as Pfizer's rule of five (RO5), was formulated in 1997 by Christopher A Lipinski for ADMET or drug pharmacokinetics to evaluate drug-likeness and the likelihood of an orally active drug with a certain pharmacological or biological activity in the human body.⁴¹ RO5 includes MW, HBD (donorHB), HBA (acptHB) and logP (QPlogPo/w) of bioactives, which are used to assess the oral availability. According to the results of Lipinski's RO5, 82.36% of the compounds synthesized in this work had no violation and 96.08% of the compounds had fewer than two violations. Figure 4 shows the frequencies of all drug-likeness criteria. According to the result of each criterion of RO5, almost all

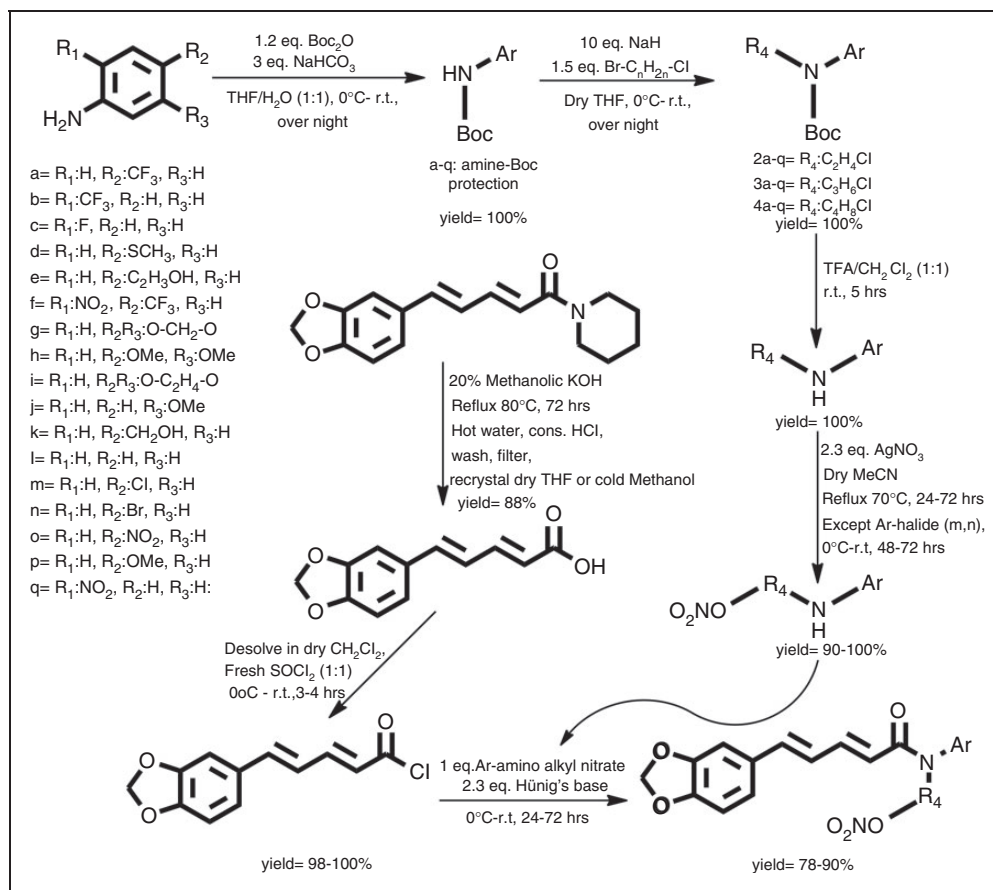


Figure 3. Methodology of the total synthetic scheme of the synthesis of piperine analogs.

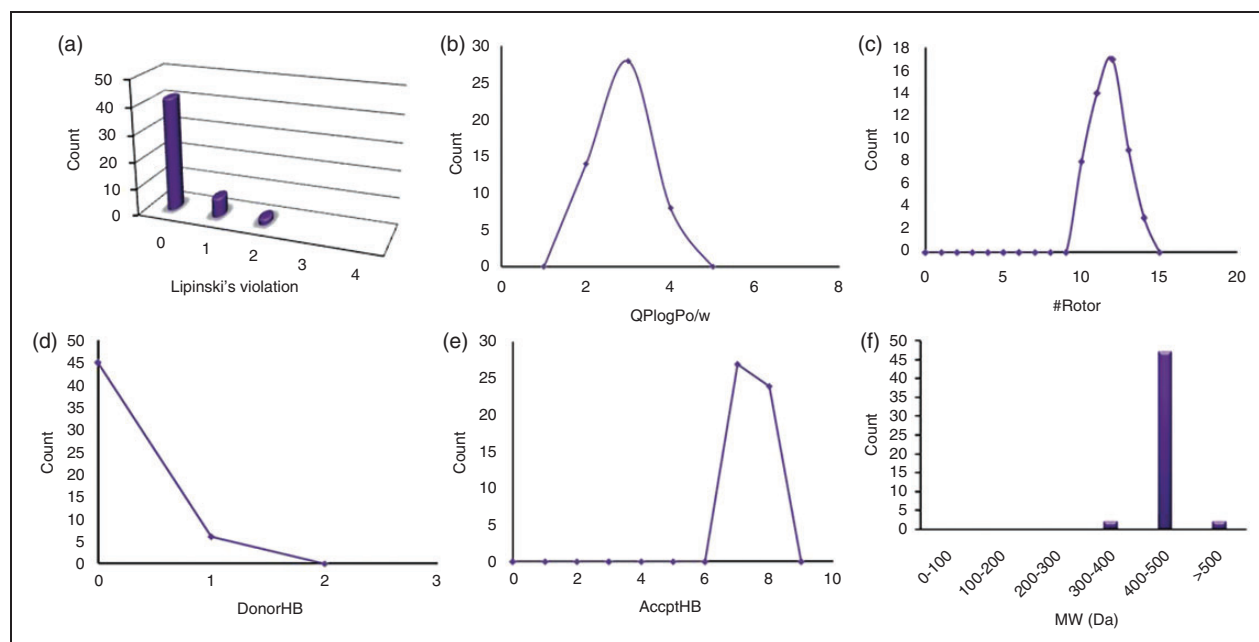


Figure 4. Drug-likeness criteria distribution graphs: (A, F) The frequencies histogram of Lipinski violations and molecular weight, and (B, C, D, E) the log P, NRB, HBA, and HBD distribution curves for all N-Aryl Piperamide NODs respectively.

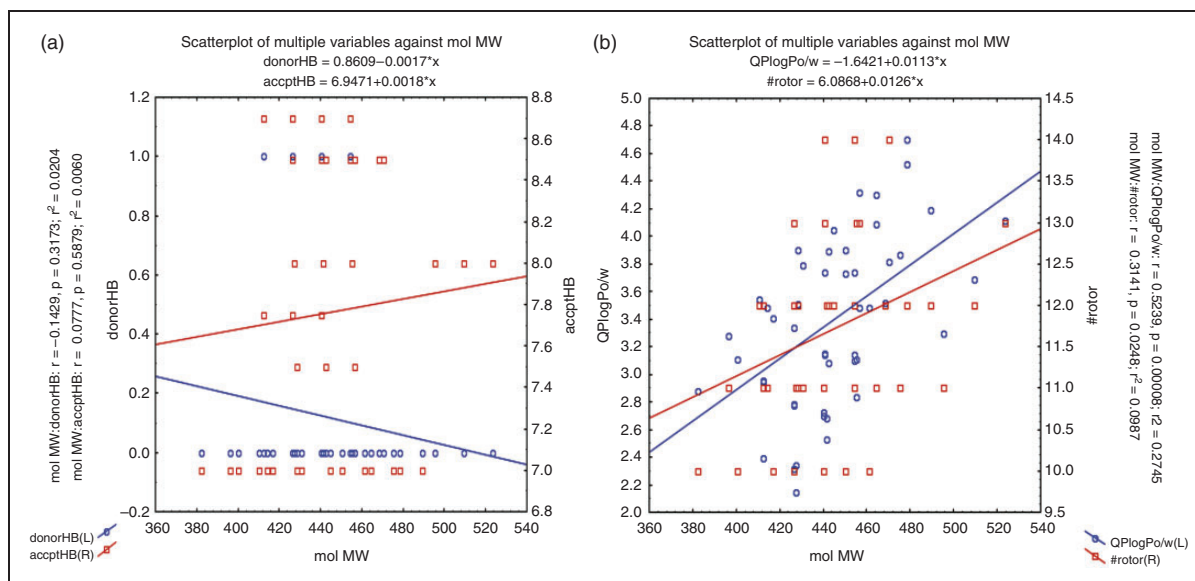


Figure 5. Multi-variation scatter plots of correlation between molecular weight (MW) and four molecular descriptors. (a) The distribution of the calculated hydrogen bond donor (donorHB) and hydrogen bond acceptor (acpctHB) vs. MW. (b) Predicted octanol/water partition coefficient (QPlogPo/w) and number of rotatable bonds (#rotor) vs. MW with R values of -0.1429 , $+0.0777$, $+0.5239$ and $+0.3141$, and P-values of 0.3173 , 0.5879 , 0.0001 and 0.0248 , respectively.

compounds were in the recommended range of the number of hydrogen bond donors, as well as hydrogen bond acceptors; 86.54% of all compounds showed no hydrogen donated by the solute to water molecules in an aqueous solution and the number of hydrogen bond acceptors fell in the range of 7–9, which was within the acceptable range. All compounds were in the recommended range (≤ 5) of the predicted octanol/water partition coefficient (QPlogPo/w) and 94.23% of all compounds possessed a molecular mass < 500 , with the number of rotatable bonds (#rotor) in the acceptable range < 15 . All RO5 criteria are depicted by double y-axis scatter plots in Figure 5(A, B). With the exception of PA-3'f and PA-4'f, all compounds were in the recommended ranges of all Lipinski criteria and could be considered drug-like.

Bioavailability

The bioavailability depends on the oral and intestinal absorption and the first-pass metabolism of the liver.⁴² The former is computed by the estimation of solubility, gut-wall permeability of the compound, ability of compound to interact with transporters across the gut-wall and metabolizing enzymes. The latter depends on the functional groups in the compound structure. The oral absorption was formulated by Jorgensen in 2000 as Jorgensen's rule of three (RO3). The RO3 includes three parameters, $\log S > -5.7$, $QPPCaco > 22$ nm/s and # primary metabolites < 7 , known as the likelihood of oral availability. $\log S$, #metab and $QPPCaco-2$ are

the parameters for prediction of aqueous solubility levels, the number of likely metabolic reactions and permeability of the gut–blood barrier (nm/s), respectively.⁴³ Qikprop employs a complex set of parameters for the prediction of bioavailability, including RO3, human oral absorption percentage, qualitative human oral absorption and the conformation-independent aqueous solubility (CIlog S), based on the similarity of compounds with their close analogs, which were practically tested. If the similarity of a designed compound and a respective known analog is < 0.9 , the Qikprop prediction is used for $\log S$ and $\log P$ (permeability prediction). Otherwise, for similarity ≥ 0.9 , the adjusted formula (1) is used for predicting the properties.

$$P_{\text{pred}} = SP_{\text{exp}} + (1 - S)P_{\text{QP}}(1)$$

P_{pred} is predicted property, S is the similarity, and P_{exp} and P_{QP} are the respective experimental and QikProp predictions for the most similar molecule within the training set. $\log P$ is predicted based on the physicochemical properties such as size, flexibility depending on the NRB,⁴³ overall lipophilicity, shape and the capacity to make hydrogen bonds.

The bioavailability of all *N*-aryl piperamide derivatives was predicted via the Qikprop module of Schrödinger suit 2011 and results are given in Table 1. The results indicated that all compounds were in the recommended ranges of $QPPCaco$ and #metab. Except PA-4'a, PA-4'e and PA-4'f, compounds

possessing logS values in an acceptable range. All showed medium-to-high levels of oral absorption based on the common parameters of the RO3, such as Clog S, percentage of oral absorption and qualitative predicted oral absorption.

The prediction of blood/brain penetration (QPlogBB)

The accessibility of druggable molecules for the CNS is an important parameter for anti-neuroinflammatory candidate drugs, which has to be considered in drug design. The blood–brain barrier (BBB) partition coefficient is a computational method for the prediction of BBB permeability to each compound.⁴⁴ Also, there are several other parameters that have to be accounted for in prediction of the BBB penetration, such as the CNS activity, logB/B and MDCK. The predicted values of logB/B indicated that all compounds fell in the acceptable range (–3.0 to 1.2).³⁴ However, according to the predicted CNS activity values, all compounds were inactive in CNS. The other important factor for mimicking BBB penetration is the non-active transportation of orally administered drugs through the Madin–Darby canine kidney (MDCK). It is due to expression of transporter protein and fewest number of metabolism enzymes.⁴⁵ The result showed that 86.27% of all compounds were within the recommended range of 25–500 nm/s.

The prediction of plasma–protein binding

The plasma makes up about 55% of the body's total volume blood. It contains various types of proteins such as lipoprotein, glycoprotein, HSA, and a, b and c globulins. The affinity of the intake drug for such proteins in plasma, known as plasma–protein binding, has a negative effect on its distribution through the blood stream and availability for its target.⁴⁶ In drug development this critical parameter has to be accounted for in evaluation of the pharmacodynamics of each designed druggable molecule. The logK_{hsa} of Qikprop is the parameter used for prediction of plasma–protein binding of a selected compound to bind to the HAS.⁴⁷ The plasma–protein binding of all designed molecules has been estimated through the Qikprop module of Schrödinger 2011 and the results indicated that all values were in the recommended range of –1.5 to 1.5.⁴⁷

Prediction of metabolism

The accessibility level of compounds for their target sites after entering the blood stream is also influenced by the number of likely metabolic reactions. The #meta of QikProp is the parameter to predict the average number of possible metabolic reactions of each

compound.³⁴ The #meta values for all compounds has been computed through Qikprop and the results showed that all compounds possessed #meta values in the recommended range of 1–8.³⁴

The prediction of blockage of human ether-a-go-go-related gene potassium (HERG K⁺) channel

One of the most important parameters for investigation of cardiac and nervous system toxicity of druggable molecules is blockage of the HERG K⁺ channel.⁴⁸ It plays an important role in the electrochemical signaling of the cardiac cycle and has a modulating function in nervous system as well. It is involved in several disorders, particularly torsade de pointes (long QT syndrome).⁴⁹ Fifty percent of the inhibitory concentration of each designed druggable molecule for HERG K⁺ channel blockage has to be computed for determination of the toxicity of compound for the cardiac as well as for the nervous system.⁴⁴ The IC₅₀ of HERG K⁺ channel blockage for each compound has been predicted via the Qikprop module of Schrödinger 2011. The results indicated that all compounds had log IC₅₀ values for blockage of HERG K⁺ channels <–5 due to donated NO. The exogenous NO stimulates the hyperpolarization-activated inward current, I_f, in the atrial and sinus tissues and is known to be neurotoxic in high doses.⁵⁰

Toxicity

Determination of drug toxicity is the cornerstone of the drugability of each designed molecule. The most important parameters for toxicity investigation are carcinogenicity, mutagenicity, EC₅₀, TD₅₀ (median toxic dose), LD₅₀, LC₅₀ (half of the lethal concentration value), weight of evidence for rodent carcinogenicity (WOE) and developmental toxicity potential (DTP). The TOPKAT approaches of Accelrys Environmental Chemistry and Toxicology Workbench have been employed to predict the ADMET profiles of all designed compounds based on the SAR of compounds in two reference drug and toxicity databases: FDA and NTP. The predicted carcinogenicity based on both databases indicated that all compounds are non-carcinogens for female mouse, female and male rat; however, 31.37% with a probability of 0.57–0.63 (NTP) and 3.91% of compounds with a probability of 0.235–0.237 (FDA) were carcinogens for the male mouse. Based on our data, around 37.25% of compounds showed skin irritancy with a probability of 0.973–0.995 and almost all caused skin sensitivity with a probability of 0.833–0.921. Also 91.17% of all compounds showed ocular irritancy with a probability of 0.97–1. Based on gentox *Salmonella* (Ames) prediction most of the compounds showed no mutagenic

activity, except 13.73% that possessed the potential to develop toxicity (DTP) with a probability of 0.49–0.56. According to WOE, compounds were devoid of carcinogenic potential in rodents. The carcinogenic TD50s of compounds were significantly high indicating the high level of safety for mice >11 and for rat > 2 mg/kg body mass/d, whereas the LD50s for orally treated rats were 0.45–8.05 g/kg body mass. The maximum tolerated doses for rats through feeding of all compounds were 0.25–3.8 and via gavages 0.000002–0.003535 g/kg body mass, whereas the EC50s (half maximal effective concentration for Daphnia Magna model) were 0.005977–0.356014 mg/l proving the great tolerances, efficacies and safeties of the designed molecules. The chronic LOAEL levels of compounds for birds in laboratory toxicity tests were 0.014–0.45 g/kg body mass. Fifty percent of inhalation lethal concentration doses of the compounds were 0.041578–1.592027 mg/m³/h. Also, 40.06% of the compounds were not aerobically biodegradable with a probability of 0.17–0.49. All toxicity profiles of compounds are given in the Supplementary Table S2.

Based on the results of ADMET studies and toxicity profiles, about 50.98% of all compounds, including PA-2'(d, e, f, i, k, o, p, q), PA-3'(d, e, i, k, o, p, q) and PA-4'(c, d, g, h, i, j, k, l, o, p, q), possessed all properties of drug-like molecules and were shortlisted for further study of their therapeutic potential as anti-neuroinflammatory agents.

Preparation of the receptors and ligands

After investigation of drugability parameters and short-listed liable candidates, drug efficacy and target affinity of compounds were computed via Schrödinger 2011. In the first step, receptors and ligands were prepared via ligprep ver. 2.5 and proprep modules of Schrödinger 2011. We have selected the NF- κ B pathway and different potential drug receptors in this pathway for screening designed compounds as anti-inflammatory agents. We have investigated the inhibitory potential of ligands against COX-2, a well-known enzyme responsible for general and neuroinflammatory diseases, and NF- κ B, which is responsible for up-stream pro-inflammatory cytokine release and initiators of inflammation. The PDB structures were downloaded from RCSB Protein Data Bank (<http://www.rcsb.org/pdb/>). Then, via the ProPrep wizard of Schrödinger 2011, protein preparation was carried out by removing the di- and trisulfide bonds of proteins, all water molecules except those that bind via hydrogen bonds with the residues in the binding side of proteins, and adding hydrogens to the molecules to satisfy the valences of the molecules. We employed OPLS 2005 force-field with RMSD 0.30. The binding sites of proteins were detected by the pose of ligands presented in receptors crystallographies, which were extracted from PDB structures.

Fifty-one different *N*-aryl piperamide NO donors have been designed and investigated for their biological activity, drugability and toxicity in comparison with a non-selective NSAID, aspirin, as the control. All ligands were prepared by using the Ligprep wizard of Schrödinger 2011 under biologically related pH using the Epik approach and OPLS2005 force-field (optimized potentials for liquid simulation force-field as a model for environmental force-field in the body).⁵¹ The stereoisomer has generated at most 32 combinations per ligand. The physiochemical properties of ligands are presented in Table S3.

Docking calculations using Schrödinger 2011

After ADME and toxicity investigation of compounds, those which possessed all parameters in the recommended range were selected for bioactivity and drug efficacy studies. The bioactivity was performed in two steps. In the first step, we investigated the effect of drugs on NF- κ B activity or complex assembly. Compounds have been selected that inhibited directly or indirectly the NF- κ B activity and translocation into the nucleus, particularly those that could bind to the Lys221 and Lys218 residues of p65 protein and protect it from acetylation. The acetylation of Lys221 and Lys 218 residues of p65 protein leads to translocation of NF- κ B into the nucleus and interaction with DNA. Prevention of acetylation of those residues can inhibit the translocation of NF- κ B and thus its activity. In the second step, the selected NF- κ B inhibitors were monitored for their potential to inhibit COX-2, either selective or non-selective.

All ADMET-approved ligands were docked in the active site of COX-2, (PDB IDs: 1CVU, 3LN1) and NF- κ B subunit p65 (PDB ID: 1NFI) via GLIDE ver. 5.5 of the Schrödinger software suite 2011. Docking was performed using extra precision (XP) docking, by adding a flexible docking option to generate conformations internally during the docking process and Epik state penalties to docking score options. The binding energies of all ligand–receptor complexes were evaluated using prime_mmgbsa ver. 1.3 and the complexes were visualized by XP visualizer module of Glide ver. 5.5, based on Glide XP_GScore.

The results indicated that out of 26 liable candidates six compounds could bind to Lys221 and Lys218 and protect them from acetylation, including PA-2'o (Lys221), PA-3'i (Lys218), PA-3'k (Lys221), PA-4'g (Lys221), PA-4'h (Lys221) and PA-4'o (Lys218). Of these, PA-3'k showed the best binding tendency towards the p65 protein with affinity value –3.503, with binding energy –41.73 kcal/mol and three hydrogen bonds to Lys221, Arg274 and Thr191, and two hydrogen bonds to Arg30 with bind distances of 1.965, 2.077, 2.084, 2.097 and 2.161 Å, respectively. Also, PA-3'k as the NO donor via modification of Cys62 by *S*-nitrosylation can inhibit the p50-DNA binding.

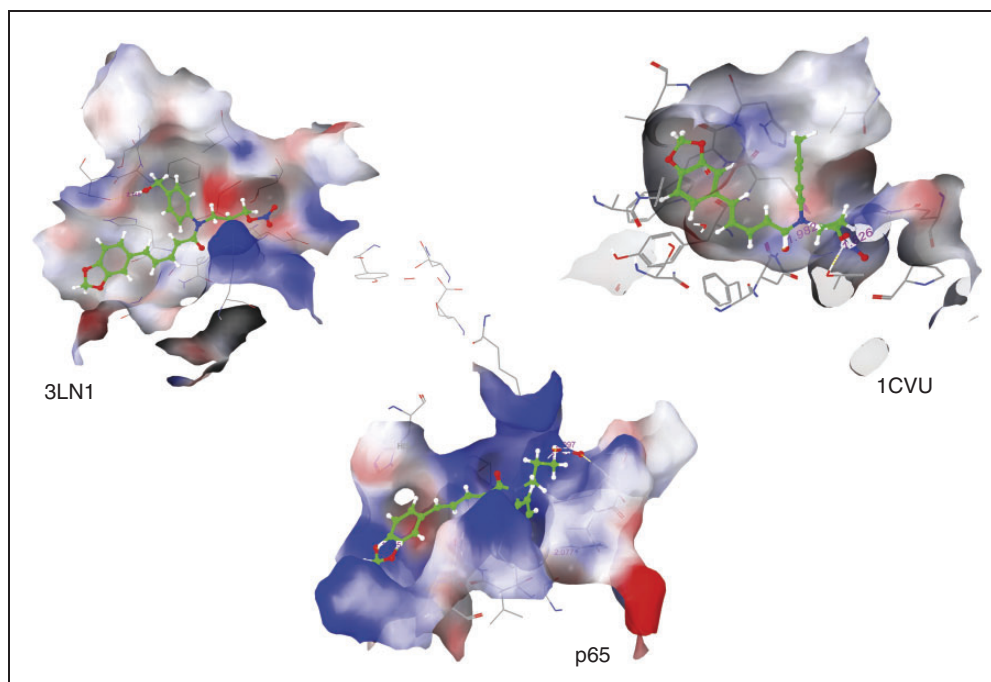


Figure 6. 3D structures of PA-3'k in the binding pockets of COX-2 (PDB IDs: 1CVU and 3LN1) and NF- κ B subunit p65 protein. The binding packet was created using the Create Binding Site Surfaces option by truncating receptor surface at 5.0 Å from the ligand, using a surface transparency of 35% with solid style and electrostatic potential color scheme.

Table 2 includes affinity values, binding energy and number of hydrogen bonds of liable candidates that passed ADME and toxicity criteria, with the active sites of receptors. Among these, PA-3'k (3-((2*E*,4*E*)-5-(benzo[d][1,3]dioxol-5-yl)-*N*-(4-(hydroxymethyl)phenyl) penta-2,4-dienamido)propyl nitrate) was the most desirable compound with the best affinity values, around -4.249 , for the inhibitory packet of COX-2 (PDB ID: 3LN) with a binding energy of -51.31 kcal/mol (close to aspirin) and -5.954 for the competitive binding side of COX-2 (PDB ID: 1CVU) with a binding energy of -53.98 kcal/mol. PA-3'k interacts with 3LN1 through one hydrogen bond to Asn567 and with 1CVU through two hydrogen bonds to Thr212 and Asn382, with bond distances of 2.146, 1.826 and 1.982 Å, respectively. The values of the XP scores, binding energies of all NO donor *N*-aryl piperamides and control compounds are presented in Table S4.

Figure 6 shows the complex of PA-3'k with the binding site of the COX-2 enzyme with both PDB IDs of 1CVU and 3LN1, and the NF- κ B subunit p65 protein, in which H-bonds are indicated with a yellow dotted line and the values of bond distances in pink. The binding packet was created by using Create Binding Site Surfaces option by truncating receptor surface at 5.0 Å from the ligand, using the surface transparency 35% with solid style and electrostatic potential colour scheme. The 2D structures of PA-3'k complexed with 3LN1 and 1CVU and p65 complexes are depicted in Figure 2(A, B), including the binding pockets residues

and chemical characterization of residues, in which the cyan, green and purple colors indicate polar, hydrophobic and positively charged amino acids, respectively. All hydrogen bonds are shown by the pink dashed line and line using for showing hydrogen bond on chain and side chain.

Experimental in vitro test

The biological experiment was performed to test the dose-dependent release of the pro-inflammatory cytokines IL-12 and IFN- γ in the extracellular matrix of human microglia (CHME3) and astrocyte (SVG) cell-lines (fourth passage) after 12 and 24 h of LPS treatment for the four selected compounds PA-2'p, PA-3'k, PA-4'g and PA-4'o by IL-12 and IFN- γ ELISA kits (Invitrogen). Also, the cell viability for both cell lines in selected doses for the four druggable candidates was evaluated by MTT assays. The results are presented in Table 3.

In neuroinflammation, IFN- γ facilitated the infiltration of T helper cells by expression of VCAM-1 and ICAM-1, and the chemokines CCL2, CXCL9 and CXCL10 in astrocytes, particularly those with close proximity to the BBB. In microglia, it gave paradoxical activities depending on the dose, pathogenic cytotoxicity or neuroprotection and apoptosis.¹⁶

Both astrocytes and microglia are able to produce biologically active IL-12p70. Because IL-12 and IL-23 share p40, astrocytes, as well as microglia, also express IL-12p35

Table 3. Biological activity of four selected N-aryl piperamides NODs in order to discover anti-neuroinflammatory drug candidates.

Title	Dose ^a	IC ₅₀ ^b			% Cell viability ^c			IL-12 quantification ^d			IFN- γ quantification ^d		
		CHME3	SVG	SVG	CHME3	SVG	SVG	CHME3	SVG	SVG	CHME3	SVG	SVG
		12	24	24	12	24	12	24	12	24	12	24	24
PA-2'p	18.59	34.13	34.98	73.23 ± 2.03	77.97 ± 1.87	113.81 ± 4.34	130.33 ± 3.47	101.88 ± 2.42	111.97 ± 2.95	57.70 ± 3.04	70.94 ± 3.41	44.46 ± 3.58	41.62 ± 2.18
PA-3'k	17.33	67.76	67.93	86.13 ± 2.57	89.13 ± 1.96	81.68 ± 4.00	101.88 ± 5.22	88.11 ± 2.80	96.37 ± 2.95	46.35 ± 3.58	54.86 ± 3.41	42.57 ± 3.58	55.81 ± 2.89
PA-4'g	3.01	8.33	8.69	81.50 ± 2.23	89.43 ± 3.23	104.94 ± 2.92	113.81 ± 3.71	90.86 ± 2.95	120.23 ± 3.47	51.08 ± 2.73	67.16 ± 3.58	57.70 ± 2.18	59.59 ± 3.04
PA-4'o	19.15	38.75	10.033	74.03 ± 4.93	95.77 ± 2.61	80.77 ± 4.34	104.63 ± 4.24	92.70 ± 3.47	111.05 ± 4.24	52.02 ± 3.58	56.75 ± 1.97	36.89 ± 2.73	45.40 ± 3.94
Disprin	9100	-	-	73.91 ± 4.93	95.55 ± 2.61	103.41 ± 3.98	114.72 ± 3.31	96.37 ± 2.95	121.15 ± 4.0	58.65 ± 3.28	69.05 ± 2.89	71.89 ± 3.94	90.81 ± 3.41
Cell+LPS	-	-	-	58.14 ± 1.39	61.09 ± 2.73	122.07 ± 4.34	151.44 ± 4.77	130.33 ± 3.47	162.45 ± 4.20	109.09 ± 2.69	125.17 ± 3.01	72.83 ± 3.82	132.43 ± 3.28

^aDoses were selected based on computed EC50.^bIC₅₀ is the half concentration of druggable compound to inhibit cell growth.^cPercentage of drug-treated inflamed cells after 24 h treatment with druggable compounds.^dPro-inflammatory cytokines estimation were performed via human IL-12 and IFN- γ ELISA kits 12 and 24 h after drug treatments.

and IL-23p19. Astrocytes express IL-12p35 mRNA constitutively, but IL-23p19 after stimulation. Thus, astrocytes, under inflammatory conditions, express all subunits of IL-12/IL-23. Via induction of IFN- γ , IL-12 activates NK cells and promotes CD4⁺ and CD8⁺ type 1 development.¹⁸ Mice with IL-12 deficiency showed IFN- γ production and defective Th1 cell responses. The active heterodimer is referred to as 'p70'. Microglia, CNS macrophages, have previously been shown to produce both the p40 and the p35 subunit of IL-12, as well as the p19 subunit of IL-23, so they are capable of Ag presentation in an IL-12/IL-23-dependent manner.¹⁸

The levels of various piperamides in different doses on secretion of IL-12 and IFN- γ 12 h after treatment with LPS, and druggable compounds are presented in Table 3. The results led to selection of four druggable molecules, PA-2'p, PA-3'k, PA-4'g and PA-4'o, with optimal doses of 18.59, 17.33, 3.01 and 19.15 ng/ml, respectively. Table 3 summarizes the selected dose of druggable molecule efficacies on cytokine expression compared with Inflamed- and market drug (Disprin)-treated cells. In most cases, PA-3'k showed better IL-12 and IFN- γ inhibitory activities. In addition, the IC50 and the percentage of cell viability of each drug are also presented in Table 3. The results of cell viabilities indicated that PA-3'k possessed best cell viability property respecting to its dose (17.33 ng/ml) with 67.76% and 67.93% of viable cells for CHME3 and SVG cell-lines, respectively.

Conclusion

NODs have a significant effect on most inflammatory disorders; however, some side effects have been reported regarding long-term treatment with NODs. The positive effects of various N-aryl piperamides have been reported and, accordingly, we have designed and screened several NO donor N-aryl piperamides *in silico*. Data indicated that among 51 compounds, 3-((2*E*,4*E*)-5-(benzo[d][1,3]dioxol-5-yl)-*N*-(4-(hydroxymethyl)phenyl)penta-2,4-dienamido)propyl nitrate with ID code PA-3'k showed the best ADME and toxicity profiles. It could inhibit the translocation of NF- κ B into the nucleus by protecting the p65 and p50 subunits of NF- κ B from acetylation via interaction with the Lys221 residue of p65 and S-nitrosylation of Cys62 of p50 using NO radical. Also, it inhibited COX-2 inflammatory function by interacting with both its substrate and inhibitory binding pockets. The affinity value of interacting with inhibitory pocket of COX-2 (PDB ID: 3LN1) was around -4.249, and the binding energy (-51.31 kcal/mol) showed a similar anti-inflammatory efficacy as aspirin. In the substrate-binding pocket of COX-2 (PDB ID: 1CVU), PA-3'k competed strongly with arachidonic acid to occupy the binding site, with an affinity value around -5.954 and a binding energy of -53.98 kcal/mol. These significant efficacies and perfect ADME and toxicity profiles made PA-3'k

an ideal candidate for an anti-inflammatory agent. Further *in vitro* and *in vivo* studies are necessary to approve the drugability of PA-3'k.

Acknowledgments

The authors are grateful to Professor Ganesh Pandey of Center for Biomedical Research, SG-PGA MS, Lucknow, Uttar Pradesh, India, for providing technical support and encouraging throughout.

Declaration of Conflicting Interests

The author(s) declared no potential conflicts of interest with respect to the research, authorship, and/or publication of this article.

Funding

The author(s) received no financial support for the research, authorship, and/or publication of this article.

References

- Trippier PC, Jansen Labby K, et al. Target-and mechanism-based therapeutics for neurodegenerative diseases: strength in numbers. *J Med Chem* 2013; 56: 3121–3147.
- Rusin A and Krawczyk Z. *Genistein derivatization-from a dietary supplement to a pharmaceutical agent*. INTECH Open Access Publisher, 2011.
- Lanas A. Role of nitric oxide in the gastrointestinal tract. *Arthritis Res Ther* 2008; 10: 1.
- Rigas B and Williams JL. NO-donating NSAIDs and cancer: an overview with a note on whether NO is required for their action. *Nitric Oxide* 2008; 19: 199–204.
- Scatena R, Bottoni P, Martorana GE and Giardina B. Nitric oxide donor drugs: an update on pathophysiology and therapeutic potential. *Expert Opin Investig Drugs* 2005; 14: 835–846.
- Tak PP, Zvaifler NJ, Green DR and Firestein GS. Rheumatoid arthritis and p53: how oxidative stress might alter the course of inflammatory diseases. *Immunol Today* 2000; 21: 78–82.
- Bao L and Xu F. Fundamental research progress of mild hypothermia in cerebral protection. *Springerplus* 2013; 2: 1.
- Ben-Neriah Y and Karin M. Inflammation meets cancer, with NF- κ B as the matchmaker. *Nat Immunol* 2011; 12: 715–723.
- Gaspar-Pereira S, Fullard N, Townsend PA, et al. The NF- κ B subunit c-Rel stimulates cardiac hypertrophy and fibrosis. *Am J Pathol* 2012; 180: 929–939.
- Qin L, Wu X, Block ML, et al. Systemic LPS causes chronic neuroinflammation and progressive neurodegeneration. *Glia* 2007; 55: 453–462.
- Qian L, Flood PM and Hong J-S. Neuroinflammation is a key player in Parkinson's disease and a prime target for therapy. *J Neural Transm (Vienna)* 2010; 117: 971–979.
- Kern TS. Contributions of inflammatory processes to the development of the early stages of diabetic retinopathy. *J Diabetes Res* 2007; 2007: 4 (Article ID 95103).
- Hess DC, Howard E, Cheng C, et al. Hypertonic mannitol loading of NF- κ B transcription factor decoys in human brain microvascular endothelial cells blocks upregulation of ICAM-1. *Stroke* 2000; 31: 1179–1186.
- Wahren J, KallasÅ and Sima AA. The clinical potential of C-peptide replacement in type 1 diabetes. *Diabetes* 2012; 61: 761–772.
- Ortuño-Sahagún D. Nitric oxide donors as neuroprotective agents after an ischemic stroke-related inflammatory reaction. *Oxid Med Cell Longev* 2013; 2013: 297357.
- Neumann M and Naumann M. Beyond I κ Bs: alternative regulation of NF- κ B activity. *FASEB J* 2007; 21: 2642–2654.
- Sprague AH and Khalil RA. Inflammatory cytokines in vascular dysfunction and vascular disease. *Biochem Pharmacol* 2009; 78: 539–552.
- Morgan MJ and Liu Z-g. Crosstalk of reactive oxygen species and NF- κ B signaling. *Cell Res* 2011; 21: 103–115.
- Mehta VB and Besner GE. Inhibition of NF- κ B activation and its target genes by heparin-binding epidermal growth factor-like growth factor. *J Immunol* 2003; 171: 6014–6022.
- Hoesel B and Schmid JA. The complexity of NF- κ B signaling in inflammation and cancer. *Mol Cancer* 2013; 12: 1.
- Bhattacharyya A, Chattopadhyay R, Mitra S and Crowe SE. Oxidative stress: an essential factor in the pathogenesis of gastrointestinal mucosal diseases. *Physiol Rev* 2014; 94: 329–354.
- Lo EH, Dalkara T and Moskowitz MA. Mechanisms, challenges and opportunities in stroke. *Nat Rev Neurosci* 2003; 4: 399–414.
- Li W, Wu S, Ahmad M, et al. The cyclooxygenase site, but not the peroxidase site of cyclooxygenase-2 is required for neurotoxicity in hypoxic and ischemic injury. *J Neurochem* 2010; 113: 965–977.
- Woyengo T, Ramprasath V and Jones P. Anticancer effects of phytosterols. *Eur J Clin Nutr* 2009; 63: 813–820.
- Esposito E and Cuzzocrea S. Antiinflammatory activity of melatonin in central nervous system. *Curr Neuropharmacol* 2010; 8: 228–242.
- Godwin P, Baird A-M, Heavey S, et al. Targeting nuclear factor- κ B to overcome resistance to chemotherapy. *Front Oncol* 2013; 3: 120.
- Zhu J, Cynader MS and Jia W. TDP-43 inhibits NF- κ B activity by blocking p65 nuclear translocation. *PLOS ONE* 2015; 10: e0142296.
- Romero A, Cacabelos R, Oset-Gasque MJ, et al. Novel tacrine-related drugs as potential candidates for the treatment of Alzheimer's disease. *Bioorg Med Chem Lett* 2013; 23: 1916–1922.
- Vasavirama K and Upender M. Piperine: a valuable alkaloid from piper species. *Int J Pharm Pharm Sci* 2014; 6: 34–38.
- Kesarwani K and Gupta R. Bioavailability enhancers of herbal origin: an overview. *Asian Pac J Trop Biomed* 2013; 3: 253–266.
- Pal Singh I and Choudhary A. Piperine and derivatives: trends in structure-activity relationships. *Curr Top Med Chem* 2015; 15: 1722–1734.
- Duffy EM and Jorgensen WL. Prediction of properties from simulations: free energies of solvation in hexadecane, octanol, and water. *J Am Chem Soc* 2000; 122: 2878–2888.
- Lipinski CA, Lombardo F, Dominy BW and Feeney PJ. Experimental and computational approaches to estimate solubility and permeability in drug discovery and development settings. *Adv Drug Deliv Rev* 2012; 64: 4–17.
- Shahbazi S, Sahrawat TR, Ray M, et al. Drug targets for cardiovascular-safe anti-inflammatory: in silico rational drug studies. *PLOS ONE* 2016; 11: e0156156.
- Friesner RA, Banks JL, Murphy RB, et al. Glide: a new approach for rapid, accurate docking and scoring. 1. Method and assessment of docking accuracy. *J Med Chem* 2004; 47: 1739–1749.
- Halgren TA, Murphy RB, Friesner RA, et al. Glide: a new approach for rapid, accurate docking and scoring. 2. Enrichment factors in database screening. *J Med Chem* 2004; 47: 1750–1759.
- Lyne PD, Kenny PW, Cosgrove DA, et al. Identification of compounds with nanomolar binding affinity for checkpoint kinase-1 using knowledge-based virtual screening. *J Med Chem* 2004; 47: 1962–1968.
- Srinivasan K. Black pepper and its pungent principle-piperine: a review of diverse physiological effects. *Crit Rev Food Sci Nutr* 2007; 47: 735–748.

39. Ahmad N, Fazal H, Abbasi BH, et al. Biological role of *Piper nigrum* L. (Black pepper): a review. *Asian Pac Trop Biomed* 2012; 2: S1945–S1953.
40. Cho H-J and Yoon I-S. Pharmacokinetic interactions of herbs with cytochrome p450 and p-glycoprotein. *Evid Based Complement Alternat Med* 2015; 2015: 736431.
41. Lipinski CA, Lombardo F, Dominy BW and Feeney PJ. Experimental and computational approaches to estimate solubility and permeability in drug discovery and development settings. *Adv Drug Deliv Rev* 1997; 23: 3–25.
42. Pond SM and Tozer TN. First-pass elimination basic concepts and clinical consequences. *Clin Pharmacokinet* 1984; 9: 1–25.
43. Shahbazi S, Kuanar A, Gade DR, et al. Semiempirical investigation of the postmenopausal breast cancer treatment potential of xanthone derivatives. *Nat Prod Chem Res* 2016; 4: 206.
44. Pajouhesh H and Lenz GR. Medicinal chemical properties of successful central nervous system drugs. *NeuroRx* 2005; 2: 541–553.
45. Ntie-Kang F, Zofou D, Babiaka SB, et al. AfroDb: a select highly potent and diverse natural product library from African medicinal plants. *PLOS ONE* 2013; 8: e78085.
46. Nicholson JP, Wolmarans MR and Park GR. The role of albumin in critical illness. *Br J Anaesth* 2000; 85: 599–610.
47. Lexa KW, Dolgih E and Jacobson MP. A structure-based model for predicting serum albumin binding. *PLOS ONE* 2014; 9: e93323.
48. Oerfi Z. Targets and off-targets of kinase inhibitors in diabetes. Dissertation, München, Technische Universität München, 2015.
49. Sanguinetti MC. HERG1 channelopathies. *Pflugers Arch* 2010; 460: 265–276.
50. Wang L. Role of nitric oxide in regulating cardiac electrophysiology. *Exp Clin Cardiol* 2001; 6: 167–171.
51. Chen I-J and Foloppe N. Tackling the conformational sampling of larger flexible compounds and macrocycles in pharmacology and drug discovery. *Bioorg Med Chem* 2013; 21: 7898–7920.